

First Ultraviolet High-Gain Harmonic-Generation Free-Electron Laser

L. H. Yu,* L. DiMauro, A. Doyuran, W. S. Graves,† E. D. Johnson, R. Heese, S. Krinsky, H. Loos, J. B. Murphy, G. Rakowsky, J. Rose, T. Shaftan, B. Sheehy, J. Skaritka, X. J. Wang, and Z. Wu

National Synchrotron Light Source, Brookhaven National Laboratory, Upton, New York 11973, USA

(Received 25 March 2003; published 14 August 2003)

We report the first experimental results on a high-gain harmonic-generation (HGHG) free-electron laser (FEL) operating in the ultraviolet. An 800 nm seed from a Ti:sapphire laser has been used to produce saturated amplified radiation at the 266 nm third harmonic. The results confirm the predictions for HGHG FEL operation: stable central wavelength, narrow bandwidth, and small pulse-energy fluctuation.

DOI: 10.1103/PhysRevLett.91.074801

PACS numbers: 41.60.Cr

There is great interest in utilizing high-gain single-pass free-electron lasers (FEL) to generate intense, short pulse radiation in the spectral region from the deep ultraviolet down to hard x-ray wavelengths [1]. The most widely studied approach has been self-amplified spontaneous-emission (SASE). In a SASE FEL [2–5], the amplifier is seeded by the shot noise in the electron beam. The SASE process produces short wavelength radiation with high peak power and an excellent spatial mode. However, the output in general has limited temporal coherence and chaotic shot-to-shot intensity variations.

An alternate approach for a single-pass FEL is high-gain harmonic-generation (HGHG) [6–8], which is capable of producing temporally coherent pulses. References to the earlier works on harmonic generation are contained in [8]. In HGHG (i) a small energy modulation is imposed on the electron beam by its interaction with a seed laser in a short undulator (the modulator) tuned to the seed frequency ω ; (ii) the resulting energy modulation is then converted into a longitudinal density modulation as the electron beam traverses a magnetic dispersion; (iii) in a second undulator (the radiator), which is tuned to the n th harmonic of the seed frequency, the microbunched electron beam emits coherent radiation at the harmonic frequency $n\omega$, which is then amplified in the radiator until saturation is reached. The output property of the HGHG FEL is a direct map of the seed laser's attributes which can have a high degree of temporal coherence. The additional benefits derived from this configuration are superior stability and control of the central wavelength, narrower bandwidth, and much smaller energy fluctuations than SASE. Furthermore, HGHG has the potential of producing light pulses that are much shorter than the electron bunch length.

The basic principle of HGHG has been demonstrated in the midinfrared using a second harmonic-generation scheme [8]. Here we report on the first operation of an HGHG FEL in the ultraviolet regime. The HGHG FEL seeded by an 800 nm laser produces saturated third-harmonic output at 266 nm. We present novel measure-

ments of the HGHG output as a function of the undulator length and demonstrate the basic principles of the process: initial coherent generation of radiation, exponential amplification, and saturation. Our experiment exhibits the key properties of HGHG radiation and demonstrates its high stability and narrow bandwidth.

Basic description of the NSLS DUV FEL—The experiments were performed on the deep ultraviolet FEL (DUV FEL) at the National Synchrotron Light Source (NSLS) of Brookhaven National Laboratory. The DUV FEL design, commissioning, and experimental details are discussed in [9–11]. The basic layout of the facility is shown in Fig. 1 and the operational parameters are as follows. The injector is a photocathode rf gun, illuminated by a frequency-tripled (266 nm) chirped pulse amplified (CPA) Ti:sapphire laser system. The rf gun produces a 300 pC, 4.5 MeV, 4 ps (FWHM) electron bunch with a normalized emittance of 3–5 μm . The four linac sections are 2.856 GHz SLAC-type. The first linac tank is set for maximum acceleration (at the rf crest) while the phase of linac tank 2 is set at 23° before the rf crest and provides an energy chirp for the bunch compressor (a four-magnet chicane) [12]. The electron energy after the first two linac tanks is 77 MeV. The third linac tank, located after the chicane, is set at a phase to remove any residual energy chirp. Linac tank 4 is operated (at the rf crest) to complete the acceleration to 177 MeV. It is also used in combination with a downstream spectrometer magnet for bunch length measurement, employing the “zero-phasing” technique [13,14].

To allow injection of the seed laser into the electron beam path, a combination of four dipole trims produces a “local bump” of the electron beam trajectory to bend the electrons around the laser seeding mirror. The energy-modulating undulator is 0.8 m long and has an 8 cm period. Its undulator parameter is $K = 1.67$ for a resonant wavelength of 800 nm and a 177 MeV electron beam. Following the modulator is a 30 cm long dispersion magnet. Next is the 10 m long near infrared scalable undulator system (NISUS) undulator [15] with a 3.89 cm period, 0.31 T peak field ($K = 1.13$), and equal focusing

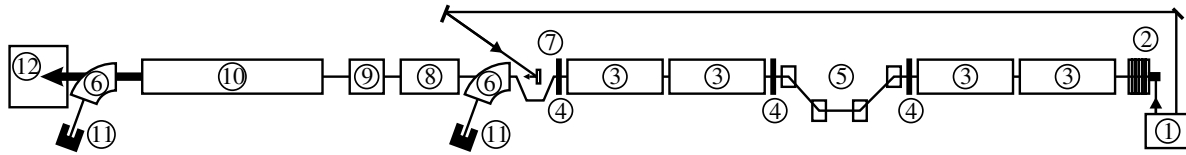


FIG. 1. The NSLS DUV FEL layout. 1: gun and seed laser system; 2: rf gun; 3: linac tanks; 4: focusing triplets; 5: magnetic chicane; 6: spectrometer dipoles; 7: seed laser mirror; 8: modulator; 9: dispersive section; 10: radiator (NISUS); 11: beam dumps; 12: FEL radiation measurements area.

in the horizontal and vertical planes by means of canted poles with 25 m betatron wavelength at 177 MeV. Each section of the long undulator is equipped with horizontal and vertical dipole correctors as well as quadrupole trims based on a 4-wire system. The electron trajectory and the transverse beam sizes ($\sim 200 \mu\text{m}$ rms) were measured using cerium-doped YAG-crystal profile monitors [16] with 20–30 μm resolution.

Experimental results.—The electron bunch length measured using the zero-phasing technique is 1 ps FWHM after compression; thus the average current within the bunch is 300 pC/1 ps = 300 A. The measured transverse normalized emittance after bunch compression is about 4.7 μm . The slice emittance [17] (the emittance within a temporal slice of the electron bunch) is slightly smaller, measured to be between 2.5 and 3.5 μm .

Using the trim dipoles the electron beam trajectory in the NISUS undulator was corrected [18] to within 200 μm peak to peak about a straight line determined by referencing the pop-in monitors to a HeNe alignment laser down the center of NISUS. The beam size as measured from the pop-in monitors provides reliable data for matching the electron beam into NISUS, and for measurement of the projected emittance, with results exhibiting excellent agreement with the emittance as measured by a quadrupole scan. The projected energy spread is 0.05% rms for the compressed bunch.

The 800 nm seed input needed for the HGHG FEL is derived from the same CPA Ti:sapphire laser system [19] that drives the photocathode rf gun but a separate optical compressor is used to produce a linearly chirped 9 ps (FWHM) seed pulse. Thus, the 1 ps electron bunch experiences only 1/9 (0.8 nm) of the total optical bandwidth. Consequently, by varying the delay of the seed pulse relative to the electron bunch, a few nanometer tuning range in the HGHG FEL output can be obtained, although not at constant seed power since the stretched seed pulse is not a flattop.

The initial synchronization between the 1 ps electron bunch and the 9 ps seed laser pulse was achieved using a streak camera after NISUS by observing both the 800 nm seed light and the 266 nm SASE light. Later, the timing was optimized using the HGHG signal as follows. For fixed values of the seed delay, wavelength, and intensity, the dispersion magnet current and the electron beam energy are varied alternately to optimize the coherently radiated power at 3 m into NISUS. For different seed

delay, this procedure is repeated until the optimized dispersion is minimized. The minimum in the dispersion corresponds to the temporal overlap between the electron bunch and the seed at its peak power.

Using the seed laser pulse duration and the measured pulse energy, we determine the seed power at the overlap between the seed pulse and the electron bunch. The seed laser's Rayleigh range is determined to be 2.4 m by spot size (400 μm rms) measurements at two monitors symmetrically located inside the modulator. These are also used to align the laser with the electron beam and to measure the electron beam size ($\sim 320 \mu\text{m}$).

As a check, we use the optimized dispersion strength to estimate the seed power. In a typical condition, when the dispersion magnet current was set at 110 A, the maximum excursion in the dispersion magnet was measured to be $x_m = 2.1$ mm by a monitor at its center, corresponding to the dispersion [7] $d\psi/d\gamma = 32\pi x_m^2 / (3s\lambda_s\gamma) \cong 5.4$, where ψ is the ponderomotive phase in NISUS, $s = 30$ cm is the dispersion section length, $\lambda_s = 266$ nm, and $\gamma = 340$ the normalized beam energy. When the dispersion is optimized for maximum bunching, i.e., maximum initial coherent generation in the first part of NISUS, the optimum dispersion value can be used to calculate the zero-to-peak energy modulation, which is found to be $\Delta\gamma = 0.5$ in the example above. Combined with the modulator parameters and the Rayleigh range, the value of the energy modulation enables us to estimate the laser power at its overlap with the electron bunch, in agreement with the more directly measured value of 30 MW.

Figure 2 shows the output pulse energy versus distance in NISUS for two different seed powers: (a) $P_{\text{in}} = 1.8$ MW and (b) 30 MW. For both cases the dispersion is varied to optimize the output power at the end of NISUS instead of 3 m into NISUS, which does not necessarily maximize the microbunching as was described above to estimate the seed laser power but results in highest HGHG output. The data were obtained using a single downstream detector and the effective NISUS length was varied by sequentially kicking the electron beam off axis using the 16 correctors uniformly distributed along its length. As a consistency check, this data was compared with a set of measurements taken by five photodiode detectors installed on the side of NISUS. Gain lengths measured by both methods agree. For $P_{\text{in}} = 1.8$ MW, $\Delta\gamma = 0.1$, and dispersion

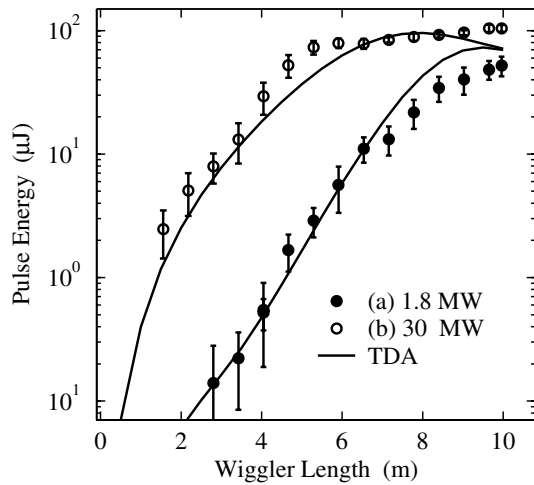


FIG. 2. Pulse energy versus distance in the radiator for two values of the seed laser input power: (a) 1.8 MW and (b) 30 MW. The solid curves are simulation results by the TDA code.

$d\psi/d\gamma = 8.7$, the gain length was found to be 0.8 m. NISUS was not engineered for DUV FEL operation, thus its parameters are not ideal for this application. Its period is longer and the electron transverse focusing is weaker than optimum. Consequently, the 10 m NISUS length and the 0.8 m gain length are inadequate to reach SASE saturation. However, there is sufficient gain to produce saturation in HGHG.

For $P_{in} = 30$ MW, $\Delta\gamma = 0.5$, and $d\psi/d\gamma = 3$, the single shot output spectrum of HGHG presented in Fig. 3 shows a line width of 0.1% FWHM. The single shot SASE spectrum with the seed laser turned off is also presented in Fig. 3. The average spacing between the SASE spectral spikes can be used to estimate the SASE pulse length [21] as $T_b = \lambda^2/0.64c\Delta\lambda = 0.9$ ps, which is close to the 1 ps electron bunch length. Notice that the HGHG spectral width of Fig. 3 is very nearly equal in width to a single spike in the SASE spectrum. This is evidence of high temporal coherence in the HGHG output.

A histogram of the shot-to-shot HGHG output pulse-energy for a 30 MW seed obtained over a minute is shown in Fig. 4, for a typical saturated output energy of 100 μ J. The rms energy fluctuation is only 7%, mostly due to shot-to-shot fluctuations and drift in the electron beam. Since the slippage of the laser pulse relative to the electron bunch over the whole NISUS (256 periods long) is 256×266 nm/c \cong 200 fs, which is 5 times smaller than the 1 ps electron pulse length, the SASE fluctuation would be $1/\sqrt{5} \cong 44\%$ for an idealized electron beam.

Analysis.—The time-independent approximation as used by the code TDA is valid, because the slippage is much smaller than the electron bunch length. Furthermore, as a rough approximation, we neglect the detailed time structure of the electron bunch. When the seed power is low, as in the 1.8 MW data of Fig. 2(a), there is a significant exponential growth along the radiator. From

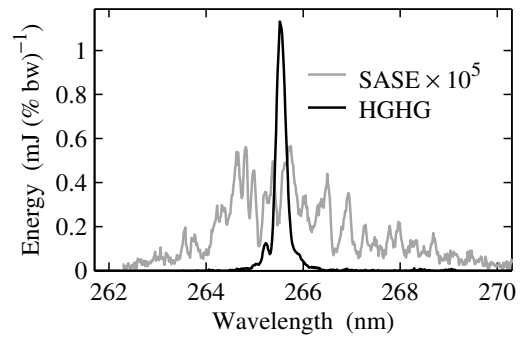


FIG. 3. Single shot HGHG spectrum for 30 MW seed power, exhibiting a 0.1% FWHM bandwidth. The gray line is the single shot SASE spectrum far from saturation when the 30 MW seed was removed. This spectrum serves as the background of the HGHG output. The average spacing between spikes is used to estimate the pulse length. The HGHG spectral brightness is 2×10^5 times larger than the SASE, because NISUS is too short to achieve SASE saturation. So this is not an appropriate comparison. If the NISUS length was doubled to 20 m, the SASE would reach saturation, but because of its broader bandwidth it would still have an order of magnitude lower brightness than the HGHG, as calculated by the code GENESIS [20].

the measured gain length of 0.8 m, we can analytically estimate the electron beam parameters. Using a 300 A current an analytical gain length calculation [22] indicates that the slice emittance is below 3 μ m, otherwise the gain length would be longer than 0.8 m. Since the measured slice emittance is between 2.5 and 3.5 μ m, the analytical solution also indicates that the local rms energy spread is smaller than the measured projected value of 5×10^{-4} . If we assume the local rms energy spread to be 1×10^{-4} and the emittance to be 2.7 μ m, the simulation by a modified TDA code [7] reproduces the measured gain length of 0.8 m and predicts the observed saturation at the end of NISUS, as shown in Fig. 2. The Pierce parameter [23] for this calculation is $\rho = 3 \times 10^{-3}$.

The 266 nm HGHG radiation pulse length in the case of the 1.8 MW seed was measured using an autocorrelator to be 0.63 ps (FWHM), which is shorter than the 1 ps electron bunch. The pulse shortening can be qualitatively

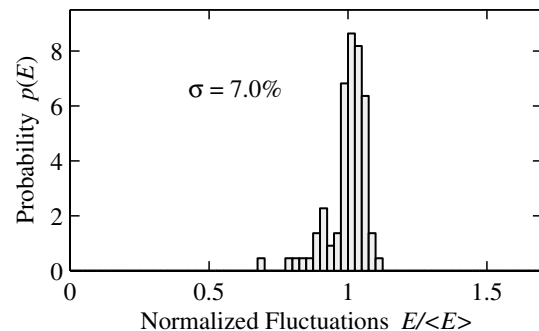


FIG. 4. Histogram of HGHG output pulse energy with 30 MW seed power.

understood as follows. The electron bunch is not flattop, so the high current part has more gain. Since there is significant exponential growth in this case of small seed power, the high current part of the bunch contributes dominantly to the output and determines the pulse length. Figure 2(a) shows that the simulated pulse energy versus distance curve for a 0.63 ps flattop pulse results in reasonable agreement with the data. In the simulation, the microbunching parameter at the beginning of NISUS is found to be $\langle \exp(i\psi) \rangle = 0.02$.

At the higher seed power of 30 MW, the autocorrelation measurement gives a pulse length of 1 ps (equal to the electron bunch length), showing that in this case the whole electron bunch contributes. For the 30 MW seed, the coherent radiated energy in the initial part of NISUS is more than a factor of 50 greater than that for the low power 1.8 MW seed, and saturation is reached at 5 m after amplifying the initial coherent radiation by only a factor of 20. This significantly reduces the required undulator length and the sensitivity of the output to electron beam parameter variation. This fact is reflected in the stable performance illustrated in Fig. 4.

Referring to Fig. 2, the analysis suggests that the observed slow growth after saturation at 5 m, rather than the drop of power as predicted by the simulation, results from the fact that the whole bunch contributes to the output, and individual slices having different currents reach saturation with different rates. Since the whole bunch is contributing to the output, part of the beam is mismatched. To approximately take this mismatch into account we use the projected emittance of $4.7 \mu\text{m}$ rather than the slice emittance in the simulation. The rms energy spread is assumed to be 1×10^{-4} . The result of the simulation, which neglects the time dependence of the electron bunch structure, shows reasonable agreement with the pulse energy versus distance data of Fig. 2(b). The microbunching parameter is for this case $\langle \exp(i\psi) \rangle = 0.1$. A more complete calculation of the experiment would require a detailed knowledge of the electron bunch structure and a time-dependent simulation.

The bandwidth within a 1 ps slice of the chirped seed is 0.8 nm (0.1% bandwidth) and the chirp in the HGHG output is expected to be the same, i.e., $0.1\% \times 266 \text{ nm} = 0.26 \text{ nm}$. This is consistent with the measured FWHM bandwidth of 0.23 nm observed in Fig. 3. A Fourier-transform limited flattop 1 ps pulse would have a bandwidth of 0.23 nm, while a FWHM 1 ps Gaussian pulse would have bandwidth of 0.1 nm.

In summary, the coherent generation and the ensuing exponential growth and saturation of an HGHG FEL operating at 266 nm has been observed and found to agree with theory. The output exhibits the predicted high stability and a nearly Fourier-transform limited bandwidth. The third-harmonic output at 88 nm accompanying the 266 nm fundamental has already been used in an ion pair imaging experiment [24] in chemical physics as its first user application [25].

This work was supported by the U.S. Department of Energy, Office of Basic Energy Sciences, under Contract No. DE-AC02-98CH10886 and by the Office of Naval Research Grant No. N00014-97-1-0845.

*Electronic address: lhyu@bnl.gov

†Present address: MIT-Bates Linear Accelerator Center, Middleton, MA 01949, USA.

- [1] S. Leone, "Report of the BESAC Panel on Novel Coherent Light Sources," U.S. Department of Energy, Washington, DC, 1999.
- [2] SLAC Report No. SLAC-R-593, edited by J. Galayda, 2002.
- [3] V. Ayvazyan *et al.*, Phys. Rev. Lett. **88**, 104802 (2002).
- [4] S.V. Milton *et al.*, Science **292**, 2037 (2001).
- [5] A. Tremaine *et al.*, Phys. Rev. Lett. **88**, 204801 (2002).
- [6] I. Ben-Zvi, L. F. Di Mauro, S. Krinsky, M. White, and L. H. Yu, Nucl. Instrum. Methods Phys. Res., Sect. A **304**, 181 (1991).
- [7] L.-H. Yu, Phys. Rev. A **44**, 5178 (1991).
- [8] L.-H. Yu *et al.*, Science **289**, 932 (2000).
- [9] L. H. Yu *et al.*, in *Proceedings of the 2001 Particle Accelerator Conference, Chicago*, edited by P. Lucas and S. Webber (IEEE, Piscataway, NJ, 2001), p. 2830.
- [10] T. Shaftan *et al.*, Nucl. Instrum. Methods Phys. Res., Sect. A **507**, 15 (2003).
- [11] A. Doyuran *et al.*, Nucl. Instrum. Methods Phys. Res., Sect. A **507**, 392 (2003).
- [12] T. Shaftan *et al.*, in *Proceedings of the European Particle Accelerator Conference, Paris, 2002*, edited by T. Garvey *et al.* (EPS-IGA and CERN, Geneva, 2002), p. 834.
- [13] D. X. Wang, G. A. Krafft, and C. K. Sinclair, Phys. Rev. E **57**, 2283 (1998).
- [14] W. S. Graves *et al.*, in *Proceedings of the 2001 Particle Accelerator Conference, Chicago* (Ref. [9]), p. 2224.
- [15] K. E. Robinson *et al.*, Nucl. Instrum. Methods Phys. Res., Sect. A **291**, 394 (1990).
- [16] W. S. Graves, E. D. Johnson, and S. Ulc, in *Beam Instrumentation Workshop*, edited by R. O. Hettel, S. R. Smith, and J. D. Masek, AIP Conf. Proc. No. 451 (AIP, New York, 1998), p. 206.
- [17] X. Qiu, K. Batchelor, I. Ben-Zvi, and X.-J. Wang, Phys. Rev. Lett. **76**, 3723 (1996).
- [18] H. Loos *et al.*, in *Proceedings of the European Particle Accelerator Conference, Paris, 2002* (Ref. [12]), p. 837.
- [19] W. S. Graves *et al.*, in *Proceedings of the 2001 Particle Accelerator Conference, Chicago* (Ref. [9]), p. 2860.
- [20] S. Reiche, Nucl. Instrum. Methods Phys. Res., Sect. A **429**, 243 (1999).
- [21] S. Krinsky and R. L. Gluckstern, Nucl. Instrum. Methods Phys. Res., Sect. A **483**, 57 (2002).
- [22] L. H. Yu, S. Krinsky, and R. L. Gluckstern, Phys. Rev. Lett. **64**, 3011 (1990).
- [23] R. Bonifacio, C. Pellegrini, and L. M. Narducci, Opt. Commun. **50**, 373 (1984).
- [24] X. Liu, R. L. Gross, and A. G. Suits, Science **294**, 2527 (2001).
- [25] W. Li and A. G. Suits (private communication).